Phase-Noise Analysis of Overlapping Filtered Multitone Waveforms in Millimeter-Wave Radio Systems

Kai Shao[1,2], Juha Yli-Kaakinen[2], Toni Levanen[2], Markku Renfors[2]

[1]Chongqing University of Posts and Telecommunications, Chongqing, China
shaokai@cqupt.edu.cn
[2]Dept. of Electronics and Communications Engineering, Tampere University of Technology, Finland
{juha.yli-kaakinen, toni.levanen, markku.renfors}@tut.fi

***Abstract*—Future wireless networks demand multicarrier modulation schemes with improved spectrum efficiency and superior spectrum containment. Orthogonal frequency-division multiplexing (OFDM) has been the favorite technique, but due to its poor spectrum containment, various alternative schemes are under consideration. This paper focuses on the filtered multitone (FMT) scheme, one of the classical filter-bank multicarrier (FBMC) schemes utilizing QAM subcarrier symbols. In contrast to OFDM and the widely-studied FBMC/OQAM, FMT does not reach maximum spectrum density of subcarriers because non-overlapping subcarriers are required to reach orthogonality. In recent work, we have studied FMT with overlapping subcarriers to reach improved spectrum density, with the conclusion that significant overlap can be tolerated, depending on the required signal-to-interference ratio. Subcarrier overlap allows to increase the roll-off of the subcarrier frequency responses, which greatly simplifies the filter-bank implementation. In this paper we investigate the effects of phase-noise, in combination with intercarrier interference introduced by the subcarrier overlap. Phase-noise is particularly critical in millimeter-wave operation, which is a central element in future systems. We show that FMT has potential for significantly improving the performance under phase-nose. Flexible fast-convolution based scheme is applied for FMT generation and receiver processing, and the tradeoffs in the parametrization of overlapping FMT are characterized using practical phase-noise models.**

***Index Terms*—filtered multitone, FMT, multicarrier, waveform, fast-convolution, physical layer, 5G-NR, phase-noise**

I. Introduction

The 5G New Radio (5G-NR) system is designed for multi-service operation with wide variety of required waveform characteristics considering, e.g., mixed numerology and asynchronous multiuser operation [1]. The waveforms and physical layer techniques at below 52.6 GHz carrier frequencies were specified in the first phase of 5G-NR development, and they are based on the orthogonal frequency-division multiplexing (OFDM) waveform with cyclic prefix (CP). While recognizing the limitations due to the poor spectrum containment of basic CP-OFDM in such scenarios, alternative spectrum enhancement schemes, mainly time-domain windowing [2] and subband-wise filtering [3], are included in the first phase of 5G physical layer development. The waveforms and physical layer techniques for mm-wave (mmW) frequences beyond 52.6 GHz will be specified in the next phases of 5G-NR development.

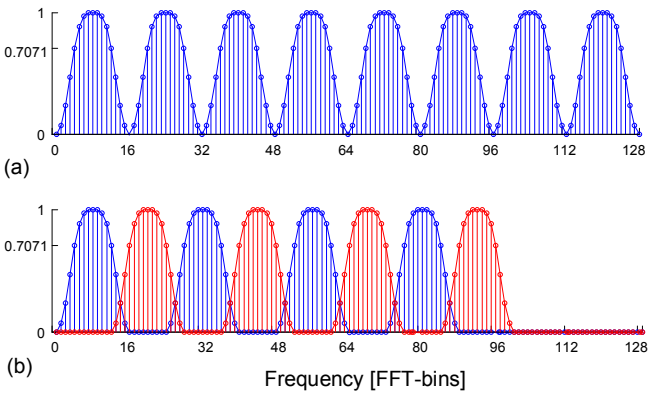

Fig. 1. FFT-domain filter weights for (a) basic FMT and (b) O-FMT.

For a multicarrier systems it is not possible to simultaneously reach (i) maximum spectrum efficiency, (ii) high spectral containment, and (iii) orthogonality of subcarriers, when using quadrature amplitude modulation (QAM) for subcarriers. The most widely-studied filter-bank multicarrier (FBMC) scheme, FBMC/OQAM, applies offset-QAM modulation to reach maximum density of orthogonal subcarriers [4]. The difficulties of OQAM modulation (e.g., in pilot-based channel estimation and in certain multi-antenna schemes) has motivated the study of non-orthogonal multicarrier schemes [5], [6].

Basically, FMT is a frequency-division multiplexing or multiple access technique, utilizing the basic Nyquist pulse-shaping principle, applied to narrow subchannels and utilizing effective uniform filter bank structure for implementation [7]. Overlapping FMT (O-FMT) aims is to improve the spectral efficiency of FMT by introducing controlled overlap of adjacent subcarriers [8], [9] (see Fig. 1). In FMT, a small roll-off means relatively narrow width of the filter transition bands

and high spectral density of subcarriers. On the other hand, it means high filter order, leading to increased complexity and long impulse response tails in transmission bursts. The overlap of FMT subcarriers compromises the orthogonality, but improves spectrum efficiency with reasonable values of roll-off and filter order. Analytical studies, confirmed by simulation results, indicated that the overlapping FMT (O-FMT) system can obtain significant spectral density improvement without requiring additional intercarrier interference (ICI) cancellation techniques [10].

Also a flexible and efficient fast convolution (FC) based waveform processing scheme [11] was proposed first in [12] for generating basic FMT and in [10] for O-FMT waveforms. It allows effective adjustment of the roll-off and subcarrier spacing to facilitate waveform adaptation in real time. FC-based O-FMT can support multicarrier operation with narrow mildly frequency-selective subcarriers, as well as multi-channel single-carrier (SC) schemes with single SC-channel per user. Mixed numerology and asynchronous uplink operation can be supported in both cases. The FC processing engine can be used for implementing frequency-domain channel equalization in both cases [10], [12], [13]. Moreover, the possibility to increase the roll-off with give spectrum density helps to reduce the peak-to-average power ratio (PAPR) of the transmitted signal in SC-operation [14].

This paper focuses on analyzing the phase-noise (PN) sensitivity of O-FMT, which is a particularly critical issue in millimeter-wave operation [15]. After introducing FC-based O-FMT in Section II, an analytical model for PN effects in O-FMT is developed in Section III. The model is verified through computer simulations using practical PN models in Section IV. In simulations we utilize the PN models developed in the mmMAGIC project [15], [16]. Then PN sensitivity of O-FMT is compared with CP-OFDM and FBMC/OQAM.

II. Fast-Convolution based O-FMT

In this paper we use a special implementation scheme for multirate filters and filter banks which is based on fast-convolution (FC) processing [11]. The main idea of FC is that a high-order filter can be implemented effectively through multiplication in frequency-domain, by multiplying bin-wise the discrete Fourier transform (DFT) of the input sequence by the precomputed DFT of the filter impulse response. Then the resulting sequence is converted back to time-domain by inverse DFT (IDFT). In practice, efficient implementation techniques, like fast Fourier transform (FFT) and inverse FFT (IFFT), are used, and overlap-save processing is applied for processing long sequences. Fig. 2 shows the basic structure of a FC based synthesis filter bank which can be used for generating O-FMT signals with flexible parametrization for different subcarriers.

The application of FC to multicarrier waveform processing was presented in [11], and the authors have introduced the idea of FC-implementation of FMT systems in [12] and O-FMT systems in [10]. With FC processing, it is possible to realize a dynamic O-FMT system, where the roll-off, subcarrier spacing, and subcarrier overlap can be adjusted in real-time based

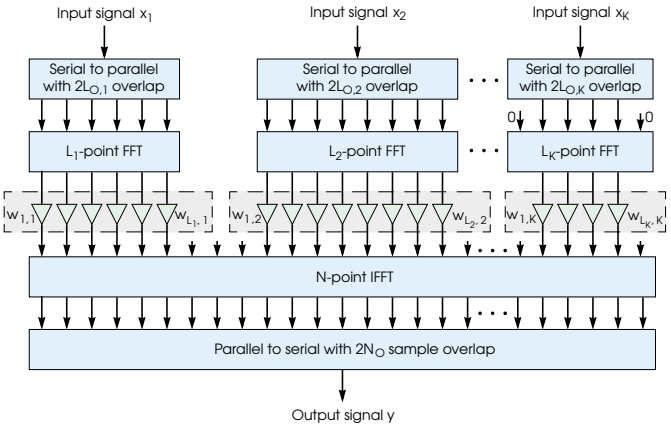

Fig. 2. Fast convolution based synthesis filter bank.

on user requirements, network load, and interference scenario. Moreover, this adjustment can be done individually for each subcarrier or group of subcarriers. Such flexibility would be quite difficult to achieve with reasonable computational complexity by time-domain filters or filter banks.

One very interesting feature of the FC structure is that the root raised-cosine (RRC) -type subchannel filters with different roll-offs can be constructed in FFT-domain in a very flexible way. This is achieved using fixed transition band weights for different subchannel bandwidths. The FFT-domain weight mask consist of two symmetric transition bands, 1-valued passband, and 0-valued stopband. The transition band weights can be obtained by frequency sampling the RRC function. Using a single prototype transition band, the roll-off factor of each subchannel can be tuned by adjusting the passband width. The subcarrier spacing can be adjusted with the resolution of FFT bin. Fig. 1 shows two examples, one with non-overlapping subcarriers, another one with the overlap of three FFT bins between adjacent subcarriers. The only difference is the center frequency of each subcarrier, which can be dynamically adjusted in FC-based implementation.

The frequency-domain weights can be designed easily by the frequency sampling approach, but better performance can be achieved by optimizing directly the weight coefficients using the ICI between subcarriers and in-band interference within each subcarrier as the performance metrics [11], [17]. With the symmetry and RRC nature of the transition bands, there are only a few free parameters in the optimization, and basic non-linear optimization methods can be used. In basic (non-overlapping) FMT, these interference effects are primarily due to circular distortion appearing when the overlap of FC processing blocks is reduced from the ideal one. Typically, overlap factors between 0.25 and 0.5 can be used to make this distortion effect small enough to be ignored when considering other imperfections of the transmission link. It was demonstrated in [10] that optimized FFT-domain weights give significant performance gain over direct RRC filter designs. Optimized weights are used also in this paper. Fig. 3 shows the signal-to-interference ratio (SIR) vs. spectral density of O-FMT with different roll-offs and overlaps.

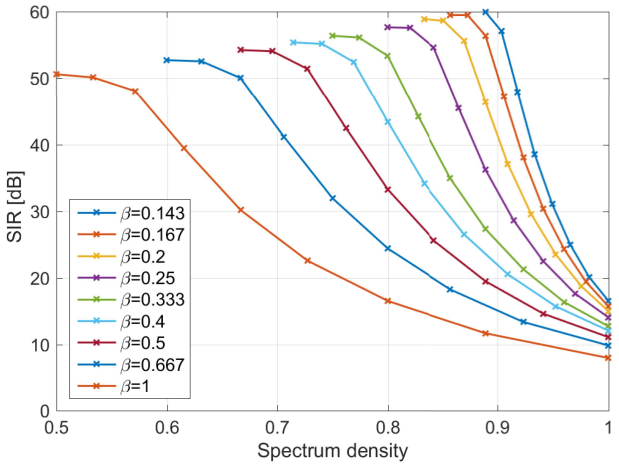

Fig. 3. SIR vs. spectrum density for O-FMT with different roll-offs β and overlaps. Here the interference is due to subcarrier overlap and small amount of inband interference due to fast-convolution processing with reduced complexity. The markers indicate the subcarrier overlap, ranging from 0 to 8 FFT bins, from left to right, respectively.

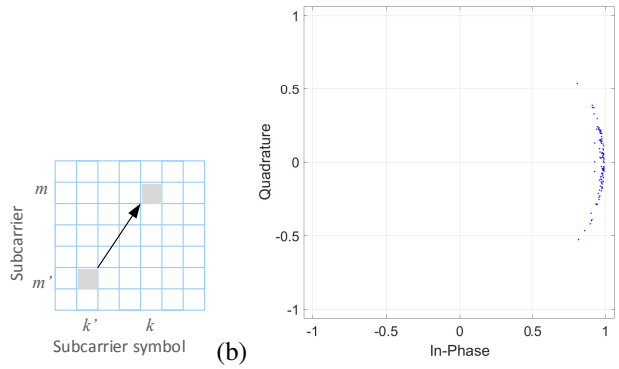

Fig. 4. Illustration of the phase-noise analysis. (a) Impulse response between subcarrier samples. (b) Common phase error term $\rho_{m,m}(k,k)$ for 100 independent O-FMT symbols obtained using the semianalytical model at 82 GHz carrier frequency with 480 kHz subcarrier spacing, $\beta = 0.25$, 4-bin overlap, and mmMAGIC high PN model.

III. Phase-Noise Analysis

Our phase-noise analysis is based on [18] addressing the basic FMT case, and [14], [19] addressing the CP-OFDM, FBMC/OQAM, and various other 5G waveform candidates.

The impulse response from k'th symbol of subcarrier m' to kth symbol of subcarrier m (illustrated in Fig. 4(a)) can be expressed as

$$p_{m',m}(k',k) = \sum_l h_{m'}(l - k'N) g_m(kN - l). \tag{1}$$

Here $h(l)$ and $g(l)$ are the transmitter and receiver prototype filters. In case of orthogonal multicarrier system,

$$p_{m',m}(k',k) = \delta(k - k') \cdot \delta(m - m'). \tag{2}$$

However, phase-noise induces both intersymbol interference (ISI) and intercarrier interference (ICI).

Let $\theta(l) = e^{j\phi(l)}$ be the complex phase-noise sequence. Then the contribution of the transmitted symbol $\alpha_{m'}(k')$ to the received symbol observation $\overline{\alpha}_m(k)$ is

$$\rho_{m',m}(k',k)\alpha_{m'}(k') = \sum_l h_{m'}(l - k'N) g_m(kN - l)\theta(l)\alpha_{m'}(k'). \tag{3}$$

Then a phase-noise distorted symbol can be expressed as

$$\begin{aligned} \overline{\alpha}_m(k) &= \sum_{m' \in M_U} \sum_{k' \in K_F} \alpha_{m'}(k')\rho_{m',m}(k',k) \\ &= \alpha_m(k)\rho_{m,m}(k,k) + \sum_{\substack{k' \in K_F \\ k' \neq k}} \alpha_m(k')\rho_{m,m}(k',k) \\ &+ \sum_{\substack{m' \in M_U \\ m' \neq m}} \sum_{k' \in K_F} \alpha_{m'}(k')\rho_{m',m}(k',k), \end{aligned} \tag{4}$$

where K_F is the set of significant subcarrier symbol indices depending on the transmission frame length, and M_U is the set of active subcarrier indices. In (4) the first term is the PN induced interference from a subcarrier symbol to itself. Typically, the subcarrier filters are obtained from a polyphase filter bank design based on a lowpass prototype filter. Since the PN sequences affecting $\rho_{m,m}(k,k)$ are equal in all subcarriers, then also these terms are equal for different subcarriers for a given value of k. This effect can be removed by dividing the symbol observations by $\rho_{m,m}(k,k)$. As indicated in the example of Fig. 4(b), $\rho_{m,m}(k,k)$ can be well approximated as a common phase rotation of the subcarrier symbols, hence it is referred to as common phase error (CPE).

The second and third terms of (4) correspond to intersymbol interference (ISI) and intercarrier interference (ICI), respectively. CPE compensation does not affect the variances of these terms. Assuming that the transmitted symbols are independent with equal variance σ_α^2, the ISI and ICI variances can be expressed as

$$\sigma^2_{\mathrm{ISI},k,m} = \sigma_\alpha^2 \cdot \sum_{\substack{k' \in K_F \\ k' \neq k}} \left|\rho_{m,m}(k',k)\right|^2 \tag{5}$$

$$\sigma^2_{\mathrm{ICI},k,m} = \sigma_\alpha^2 \cdot \sum_{\substack{m' \in M_U \\ m' \neq m}} \sum_{k' \in K_F} \left|\rho_{m',m}(k',k)\right|^2. \tag{6}$$

Naturally, at the edges of the active subcarrier allocation the ICI term is reduced somewhat, and at the beginning and end of the transmission frame (assuming guard period between transmisison frames), the ISI term is reduced somewhat. But for most of the subcarrier symbols, the PN interference can be considered equal, also in link error rate analysis.

In [18] link error rate analysis was carried out based on simplified model of the PN spectrum and analytical model for the PN effects. We leave the corresponding analysis for O-FMT as a topic for future studies. Instead, we calculate the ISI and ICI terms of (4) using PN sequences obtained from a phase-noise simulator. The developed semianlytical model gives effective tools for O-FMT system parametrization and it also gives insight about the significance of ISI and ICI terms of the PN distortion.

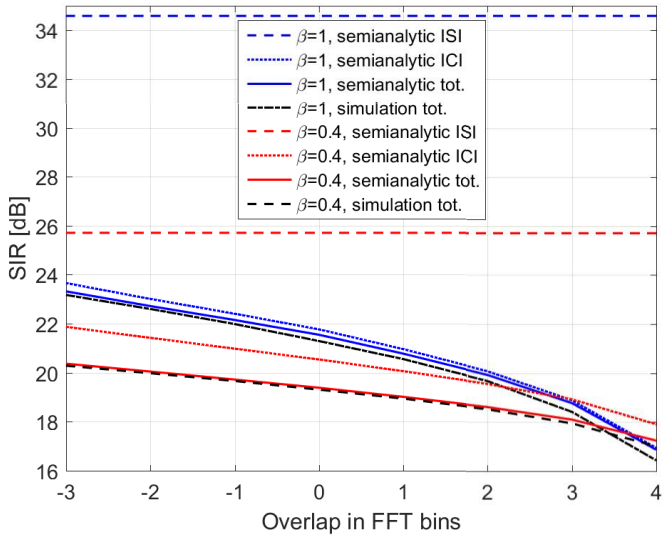

Fig. 5. SIR vs. subcarrier overlap based on the semianalytical model and simulations using mmMAGIC high PN model at 82 GHz carrier frequency with 1.92 MHz subcarrier spacing and roll-offs of $\beta = \{1, 0.4\}$.

IV. Simulation Results

We consider the same carrier frequencies as in [15], 28 GHz and 82 GHz, together with the mmMAGIC low and mmMAGIC high PN models for the receiver local oscillator. Ideal noise-free channel and perfect compensation of the common phase error (CPE) are assumed in the following results (in the same way as in [14]). Thus the results indicate the upper limit for the practical link performance.

Fig. 5 shows a comparison of SIR performance based on the semianalytical model and simulations at 82 GHz carrier frequency using the mmMAGIC high phase-noise model. The subcarrier spacing is 1.92 MHz and 300 active subcarriers are assumed with roll-offs of $\beta = 1$ and $\beta = 0.4$. The simulation results are obtained with 4000 O-FMT symbols. The semianalytical results are obatained by limiting the ICI effects to eight adjacent subcarriers on both sides and averaging the results over 100 independent PN sequences. It can be seen that the semianalytical model matches rather well with simulations. ICI dominates the performance in all considered cases. The ISI term is almost independent of overlap, and it becomes more significant with small roll-off values.

Fig. 6 shows the SIR vs. spectral density for O-FMT with different roll-off and overlap values. In Fig. 3 the upper limit of SIR (at about 50-60 dB level) is due to the inband interference caused by FC processing with FC overlap factor of 0.5, while in Fig. 6, the upper limit is due to receiver phase-noise. We can see that significant amount of subcarrier overlap can be accepted without performance loss.

Figs. 7, 8, and 9 show the achievable SIR vs. spectrum density for different subcarrier spacings (SCSs) and selected roll-off values. In this context, negative overlap values indicate cases where additional guarbands are introduced between the subcarriers. The corresponding results are shown also for CP-OFDM and FBMC/OQAM, both having the maximum density

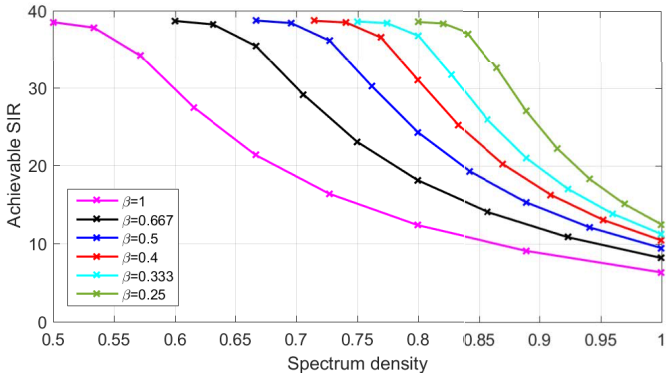

Fig. 6. SIR vs. spectrum density for O-FMT with different roll-offs β and overlaps. Here the interference is due to subcarrier overlap and receiver PN with mmMAGIC low PN model. Carrier frequency of 28 GHz and 480 kHz subcarrier spacing. The markers indicate the subcarrier overlap ranging from 0 to 8 FFT bins, from left to right, respectively. Big markers indicate cases of 0-overlap.

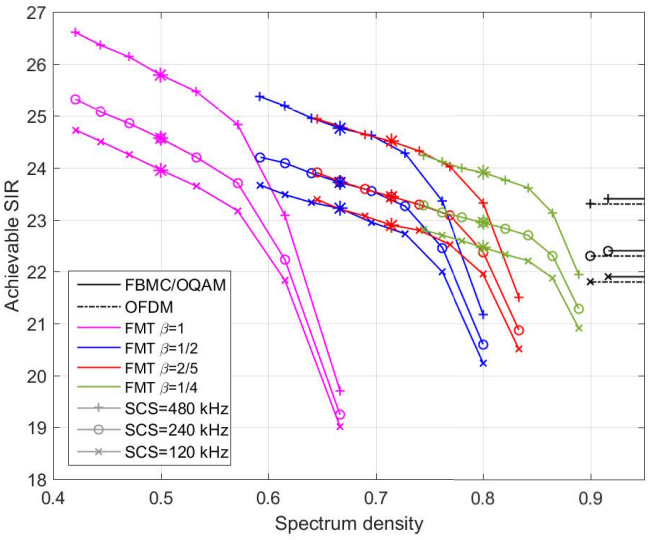

Fig. 7. Achievable SIR vs. spectrum density for different overlaps at 28 GHz carrier frequency and mmMAGIC high PN model. Markers indicate overlaps from -3 to 4 FFT bins, from left to right.

of subcarriers. With these reference systems, the overheads in spectrum density are due to guardbands. With CP-OFDM, also the CP overhead reduces the spectrum utilization, but this effect is not included in the figures. FMT has the capability for considerably reduced PN sensitivity, at the cost of reduced spectrum density. We can also see that O-FMT allows to significantly increase the roll-off of the subchannel filters without loss in the SIR performance. One example case is that with 82 GHz carrier frequency and mmMAGIC high PN model (Fig. 9), the roll-off $\beta = 0.4$ with 3 bin overlap reaches the same spectrum density and the same or slightly higher SIR than the roll-off $\beta = 0.25$ without overlap. This applies for all considered subcarrier spacings. This helps to significantly reduce the peak-to-average power ratio (PAPR) of the transmitted signal and also reduce the implementation complexity [14].

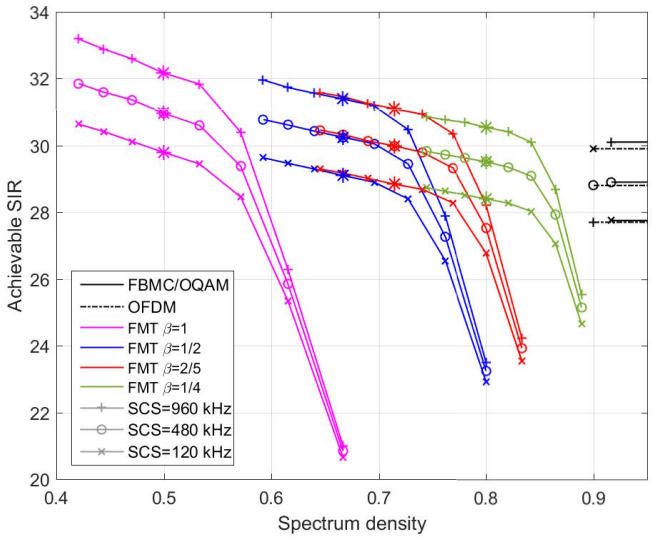

Fig. 8. Achievable SIR vs. spectrum density for different overlaps at 82 GHz carrier frequency and mmMAGIC low PN model. Markers indicate overlaps from -3 to 4 FFT bins, from left to right.

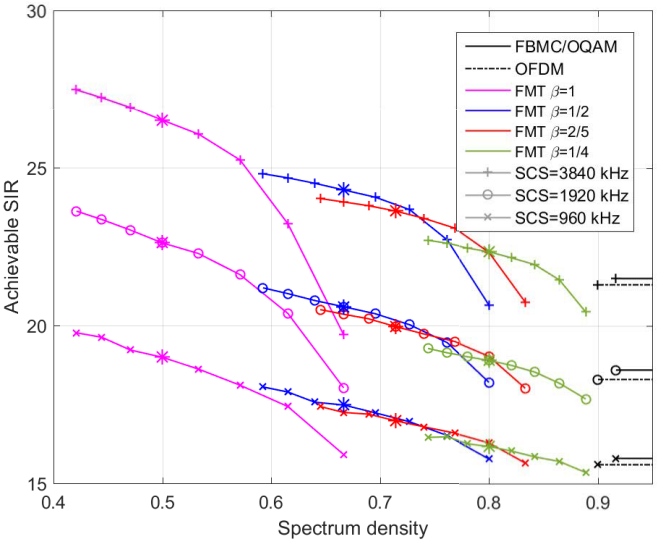

Fig. 9. Achievable SIR vs. spectrum density for different overlaps at 82 GHz carrier frequency and mmMAGIC high PN model. Markers indicate overlaps from -3 to 4 FFT bins, from left to right.

V. Concluding Remarks

We can conclude that fast-convolution based implementation of O-FMT offers high flexibility as a multicarrier modulation scheme and also as pulse-shaping and multiplexing/multiple access scheme in single-carrier transmission at mmW bands. Different users' subbands (groups of subcarriers) can be configured for different roll-offs and subcarrier overlaps. Then the sensitivity to phase-noise can be adjusted based on the requirements of the modulation and coding scheme applied for each user. For high-rate MCS, O-FMT has potential for considerably reduced PN effects compared to CP-OFDM. Subcarrier overlap makes it possible to increase the filter roll-off, resulting in reduced complexity and reduced PAPR in SC transmission with acceptable interference level due to PN.

References

[1] M. Shafi, A. F. Molisch, P. J. Smith, T. Haustein, P. Zhu, P. D. Silva, F. Tufvesson, A. Benjebbour, and G. Wunder, "5G: A tutorial overview of standards, trials, challenges, deployment, and practice," *IEEE J. Select. Areas Commun.*, vol. 35, no. 6, pp. 1201–1221, June 2017.

[2] R. Zayani, Y. Medjahdi, H. Shaiek, and D. Roviras, "WOLA-OFDM: A potential candidate for asynchronous 5G," in *IEEE Globecom Workshops (GC Wkshps)*, Dec. 2016, pp. 1–5.

[3] J. Yli-Kaakinen, T. Levanen, S. Valkonen, K. Pajukoski, J. Pirskanen, M. Renfors, and M. Valkama, "Efficient fast-convolution-based waveform processing for 5G physical layer," *IEEE J. Select. Areas Commun.*, vol. 35, no. 6, pp. 1309–1326, Jun. 2017.

[4] P. Siohan, C. Siclet, and N. Lacaille, "Analysis and design of OFDM/OQAM systems based on filterbank theory," *IEEE Trans. Signal Processing*, vol. 50, no. 5, pp. 1170–1183, May 2002.

[5] R. Zakaria and D. L. Ruyet, "On maximum likelihood MIMO detection in QAM-FBMC systems," in *Proc. IEEE Int. Symp. Pers., Indoor, Mobile Radio Commun.*, Sept 2010, pp. 183–187.

[6] Y. H. Yun, C. Kim, K. Kim, Z. Ho, B. Lee, and J. Seol, "A new waveform enabling enhanced QAM-FBMC systems," in *Proc. IEEE Works. on Sign. Proc. Adv. in Wirel. Comms.*, June 2015, pp. 116–120.

[7] G. Cherubini, E. Eleftheriou, and S. Olcer, "Filtered multitone modulation for very high-speed digital subscriber lines," *IEEE J. Select. Areas Commun.*, vol. 20, no. 5, pp. 1016–1028, June 2002.

[8] S. Tomasin and A. Zaidi, "Precoded filtered multitone with overlapping subcarriers for 5G communication systems," in *2015 5th International Conference on Communications and Networking (COMNET)*, Nov 2015, pp. 1–6.

[9] M. H. Ylmaz and H. Arslan, "Resource allocation with partially overlapping filtered multitone in cognitive heterogeneous networks," *IEEE Commun. Lett.*, vol. 20, no. 5, pp. 962–965, May 2016.

[10] K. Shao, L. Pi, J. Yli-Kaakinen, and M. Renfors, "Filtered multitone multicarrier modulation with partially overlapping sub-channels," in *Proc. European Sign. Proc. Conf.*, Aug 2017, pp. 405–409.

[11] M. Renfors, J. Yli-Kaakinen, and F. Harris, "Analysis and design of efficient and flexible fast-convolution based multirate filter banks," *IEEE Trans. Signal Processing*, vol. 62, no. 15, pp. 3768–3783, Aug. 2014.

[12] K. Shao, J. Alhava, J. Yli-Kaakinen, and M. Renfors, "Fast-convolution implementation of filter bank multicarrier waveform processing," in *Proc. IEEE Int. Symp. Circuits and Systems*, Lisbon, Portugal, May 24–27 2015, pp. 978–981.

[13] M. Renfors and J. Yli-Kaakinen, "Channel equalization in fast-convolution filter bank based receivers for professional mobile radio," in *Proc. European Wireless*, Barcelona, Spain, May 14–16 2014.

[14] J. Luo et al., "Final radio interface concepts and evaluations for mm-wave mobile communications," Project mmMAGIC (Millimetre-Wave Based Mobile Radio Access Network for Fifth Generation Integrated Communications) Deliverable D4.2, Jun. 2016. [Online]. Available: https://bscw.5g-mmmagic.eu/pub/bscw.cgi/d214055/mmMAGIC_D4.2.pdf

[15] Y. Zou, P. Zetterberg, U. Gustavsson, T. Svensson, A. Zaidi, T. Kadur, W. Rave, and G. Fettweis, "Impact of major RF impairments on mm-wave communications using OFDM waveforms," in *2016 IEEE Globecom Workshops (GC Wkshps)*, Dec 2016, pp. 1–7.

[16] P. Zetterberg et al., "Initial multi-node and antenna transmitter and receiver architectures and schemes," Project mmMACIG (Millimetre-Wave Based Mobile Radio Access Network for Fifth Generation Integrated Communications) Deliverable D5.1, Mar. 2016. [Online]. Available: https://bscw.5g-mmmagic.eu/pub/bscw.cgi/d95056/mmMAGIC_D5_1.pdf

[17] J. Yli-Kaakinen and M. Renfors, "Optimized reconfigurable fast convolution based transmultiplexers for cognitive radio," *IEEE Trans. Circuits Syst. II*, vol. 65, no. 1, pp. 130–134, Jan. 2017.

[18] N. Moret and A. M. Tonello, "Performance of filter bank modulation with phase noise," *IEEE Trans. Wireless Commun.*, vol. 10, no. 10, pp. 3121–3126, October 2011.

[19] J. Luo et al., "Preliminary radio interface concepts for mm-wave mobile communications," Project mmMACIG (Millimetre-Wave Based Mobile Radio Access Network for Fifth Generation Integrated Communications) Deliverable D4.1, Jan. 2016. [Online]. Available: https://bscw.5g-mmmagic.eu/pub/bscw.cgi/d127361/mmMAGIC_D4.1.pdf